

# Acoustic Transmissibility of Advanced Turboprop Aircraft Windows

Ferdinand W. Grosveld\*

*Planning Research Corporation, Hampton, Virginia*

The transmissibility of two triple-pane windows, designed to provide 69-dB noise transmission loss at the blade propeller frequency of an advanced turboprop aircraft (164 Hz), was investigated experimentally using insertion loss and three-dimensional intensity techniques. Experimental modal analysis was performed to determine pane modal frequencies, and double/triple wall and lump mass resonance frequencies. Due to the lack of stiffness at the window boundaries and the presence of lump mass resonances, the transmission loss of the windows was limited to their mass law in the frequency range of interest (125–630 Hz). Double/triple wall resonances were found to degrade the transmission loss of each of the two windows. It was shown that, at the blade passage frequency and the first two overtones, combinations of window plus scratch shield provide less transmission loss than the average transmission loss of the treated fuselage. Considerable disagreement was obtained between the experimental transmission loss of this investigation and the theoretical predictions from another study, partly because of assumptions in the theory that could not be reproduced in the laboratory setup.

## Introduction

ADVANCED turboprop propellers are expected to generate higher exterior noise levels than the propeller design on current aircraft. Acceptable cabin noise levels for these advanced turboprop aircraft can be achieved by using appropriate fuselage sidewall designs.<sup>1,2</sup> For an efficient sidewall design, the window and supporting wall would need to have the same acoustic transmission characteristics at the critical turboprop frequencies. An analytical and parameter design study was performed in Ref. 3, resulting in two triple-pane window configurations that would provide 69 dB noise transmission loss at an estimated blade passage frequency of 164 Hz. This would reduce the peak external surface sound pressure level of 150 dB to an acceptable 75 dBA inside the cabin. Acoustic transmissibility of aircraft-type windows has been addressed in several publications,<sup>4–7</sup> but no experimental data were available for the triple-pane window designs of Ref. 3. The purpose of this article is to report on the transmissibility of the two triple-pane window configurations,<sup>3</sup> relate their transmission loss to that of an appropriately designed sidewall,<sup>1,2</sup> and compare the experimental results with transmission loss predictions. The primary frequency range of interest covers the one-third octave bands 125–630 Hz, which include the blade passage frequency and three harmonics. Data are presented up to the 1000 Hz one-third octave band to show the trend of the data just above the frequency range of interest.

## Window Designs

The aluminum frames of the window designs measure  $31.8 \times 39.4 \times 5.6$  cm and contain three  $25.4 \times 33.0$ -cm window panes with a transparent area of  $21.6 \times 29.2$  cm. A picture of one of the windows is shown in Fig. 1. The heaviest of the two windows is designated window I and has a total surface density of  $51.7 \text{ kg/m}^2$ . Two of the three panes are made of 0.94-cm-thick glass and separated by an airspace of 0.79 cm. The third pane, which is made of acrylic for safety considerations, is 0.64 cm thick and is separated from one of

the glass panes by a 2.54-cm airspace. When the window is installed, the acrylic pane faces the inside of the fuselage cabin. Window II, with a surface density of  $44.9 \text{ kg/m}^2$ , has the same configuration as window I except that the glass pane in the middle is replaced by a 0.64-cm-thick glass pane, while preserving the spacing with the other glass pane. The panes are supported by strips of elastomer kept in place with a contact cement. Silicon rubber is used to secure the windows in a 6.4-cm-deep aluminum frame. A sketch of the window I configuration is shown in Fig. 2.

## Window Resonance Frequencies

System resonance frequencies adversely affect the transmission loss characteristics of the triple-pane window. For the window designs in the current investigation, three types of resonances were found to be important:

- 1) Single-pane modal resonances, where the vibrational response of the pane is decomposed into mode shapes with characteristic modal damping and modal frequency;
- 2) Double and triple wall resonances, where the fluid between two panes acts as a spring and the vibration of two opposing panes is out of phase; and
- 3) Lump mass resonances, where the bulk of the window including the frame is resonating. The boundary conditions – the way in which the window is supported – determine the stiffness and damping of the system.

Simple calculations showed that coincidence and cavity resonances occur well above the frequency range of interest. To determine single-pane modal resonances, a modal analysis was performed using transfer functions between impulse excitation by a force-gage-equipped hammer and the acceleration response of the pane at several locations on the pane surface. For these experiments, the windows were supported by rubber strips underneath the aluminum frame. Modal parameters were extracted by curve fitting circles through data points of modulus/phase polar (Nyquist) plots of the frequency-response functions. The resulting modal frequencies and damping in the frequency range of interest are tabulated in Table 1 for the surface panes of windows I and II.

The modal frequencies of the three window panes were calculated for simply supported boundary conditions with<sup>8</sup>

$$f_{l,n} = \frac{\pi}{2} \left[ \frac{Et^2}{12(1-\nu^2)m} \right]^{1/2} \left[ \left( \frac{l}{a} \right)^2 + \left( \frac{n}{b} \right)^2 \right] \quad (1)$$

Presented as Paper 87-2662 at the AIAA 11th Aeroacoustics Conference, Sunnyvale, CA, Oct. 19–21, 1987; received Oct. 20, 1987; revision received April 12, 1988. Copyright © 1987 American Institute of Aeronautics and Astronautics, Inc. All rights reserved.

\*Aerospace Research Engineer. Associate Fellow AIAA.

Table 1 Calculated and measured window resonance frequencies

Resonance system	Material	Thickness, cm	Mode	Calculated (Simply supported)	Experimental			
				Frequency, Hz	Window I Frequency, Hz	Window I Damping factor	Window II Frequency, Hz	Window II Damping factor
Single pane	Acrylic	0.64	1,1	126	—	—	—	—
			1,2	266	283	0.0243	261	0.0154
			2,1	363	384	0.0149	379	0.0129
			1,3	500	—	—	—	—
	Glass	0.94	1,1	558	557	0.0275	585	0.0154
Double/triple wall	Acrylic/glass glass	0.64	1,1	380	—	—	—	—
				128–226 <sup>a</sup>	196	0.0252	183	0.0238
					516	0.0160	472	0.0309
Lump mass	Complete window				65	0.0604	69	0.1129

<sup>a</sup>Range of frequencies for double wall resonances.

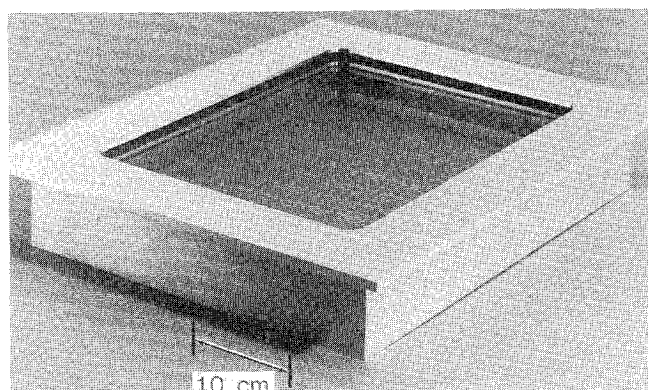


Fig. 1 Window design for the advanced turboprop aircraft.

where  $t$  is the thickness,  $m$  is the surface density, and  $a$  and  $b$  are the width and length of the window panes. Young's modulus  $E$  and Poisson's ratio  $\nu$  for the acrylic pane were taken as  $0.31 \times 10^{10}$  N/m<sup>2</sup> and 0.4. For the glass panes, these material properties were  $6.2 \times 10^{10}$  N/m<sup>2</sup> and 0.24. As shown in Table 1, reasonable agreement is obtained between calculated and experimental values of the 1,2 and 2,1 modes of the acrylic pane and the fundamental mode of the outer glass pane. This suggests that the boundary conditions with the panes supported as shown in Fig. 2 are approximated closely by simply supported conditions. The inner glass pane was not accessible for analysis.

To obtain double/triple wall and lump mass resonances, transfer functions in the form of Bode diagrams were obtained by relating impulse excitation and normal acceleration response of the two outer panes and the window frame. For that purpose, accelerometers were attached to the centers of the acrylic pane and the glass pane and to one of the corners of the aluminum frame. Figure 3 shows the relative magnitude of a transfer function between the response of an accelerometer in the center of the acrylic pane of window I and the input of an impact hammer right next to it. This transfer function exhibits dominant responses at 196 and 516 Hz. Similarly, dominant relative magnitudes were found at 183 and 472 Hz for window II. These resonances and their damping factors are tabulated in Table 1. Also in this table is the range of calculated double wall frequencies for combinations of two panes with the third pane omitted. Because of the strong response of these resonances, the modal parameters of the 1,1 and 1,3 modes of the acrylic pane could not be extracted. To verify that these resonances were of the double/triple wall type, the phase dif-

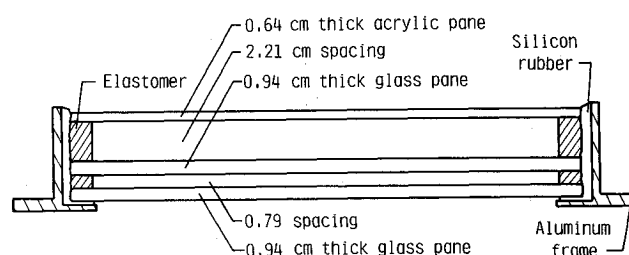


Fig. 2 Lengthwise cross section of window I.

ference and the coherence between the acceleration signals were measured to obtain their linear causality. Lump mass resonances were found at 65 and 69 Hz for windows I and II, respectively.

## Window Transmission Loss

### Predictions

A theoretical parameter study was performed in Ref. 3 to establish specifications for acoustic window designs for advanced turboprop-powered aircraft. The study was based on the approach taken in Ref. 9, in which the transmission loss was calculated from the pressure ratio across the multilayered configuration expressed in terms of the pressure ratio across the individual layers. This pressure ratio can be calculated if both the characteristic and termination impedances of the layers are known. The parametric studies were performed for normal sound incidence conditions. Over 200 configurations for a multiple-pane design were analyzed, and the designs of windows I and II were selected. The predicted transmission losses of these window designs with and without a scratch shield installed are depicted graphically in Fig. 4. Indicated in this figure are the fundamental blade frequency (164 Hz) and the second (328 Hz) and third harmonics (492 Hz). Although not indicated in the figure, the fourth harmonic (656 Hz) is within the frequency region of interest. These harmonics appear in the 160-, 315-, 500-, and 630-Hz one-third octave bands, respectively.

### Measurements

Measurements were carried out in the NASA Langley Research Center Transmission Loss Apparatus.<sup>10</sup> (See Fig. 6.) The double wall that contains the test specimen and separates the receiving and source rooms was modified through the addition of lead, concrete, and other mass treatment to provide an estimated 57 dB transmission loss at 160 Hz, which is the equivalent of a 50-cm-thick concrete wall. To increase transmission loss at higher frequencies, 1-ft-thick foam blocks were

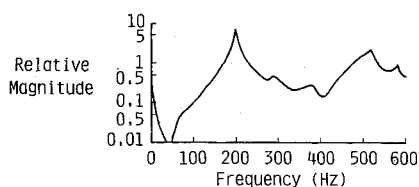


Fig. 3 Relative magnitude of transfer function between hammer impulse excitation and accelerometer response in center of the window I acrylic outer pane.

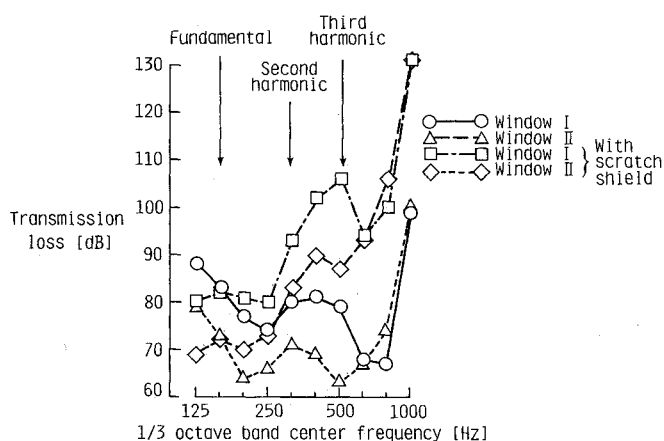


Fig. 4 Transmission loss predicted for triple-pane window designs.<sup>3</sup>

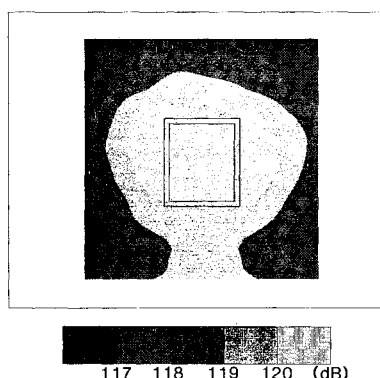


Fig. 5 Sound pressure level distribution on the source side of the fuselage panel.

inserted to fill the space between the walls of the receiving and source rooms. The background noise in the receiving room was measured to be less than 35 dB in each one-third octave band in the frequency range of 125–1000 Hz. Because of the size of the window designs, the layout and size of the source and receiving rooms, the frequency range of interest, and the expected high transmission loss of the windows, it was not possible to test these windows according to the standard of the American Society for Testing Materials.<sup>11</sup> The transmission loss of the two windows was determined from insertion loss measurements in a fashion similar to the method described in Ref. 10. The transmission loss of the windows when installed in a fuselage sidewall panel was obtained by intensity measurements because the insertion loss method was unable to distinguish noise transmission through the fuselage panel and noise transmitted through the window. Both methods are compared to one another and to mass law transmission loss. Excitation was provided by a pneumatic horn located 1.3 cm from the test specimen, yielding a sound pressure level distri-

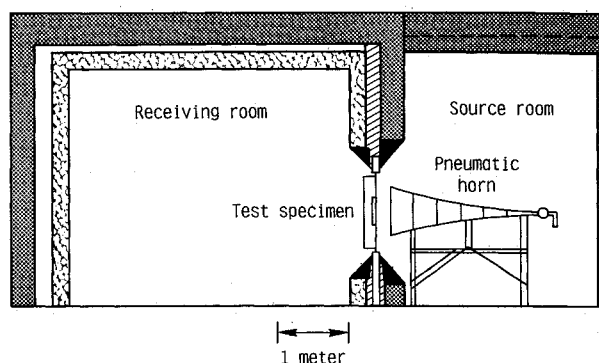


Fig. 6 Test configuration in the NASA Langley Research Center Transmission Loss Apparatus.

bution on the source side as depicted in Fig. 5. This arrangement provided the best possible approximation to the normal sound incident condition employed in Ref. 3. The exponential horn is 2.13 m long with a mouth diameter of 0.61 m and a flare constant of  $2.60 \text{ m}^{-1}$ . The horn is driven by low-pressure air (40 psi) in combination with a white noise generator. Its cutoff frequency is calculated to be at 71 Hz. The test configuration is depicted in Fig. 6.

#### Insertion Loss

**Test configuration.** In the opening between the two rooms, a 8.9-cm-thick particle board panel ( $1.22 \times 1.52 \text{ m}$ ) was installed to support either one of the window designs. The particle board insert was of much higher surface density ( $82.9 \text{ kg/m}^2$ ) than the window designs, exhibiting an inherently higher transmission loss in the mass-controlled frequency region. This should minimize possible contributions from sound reaching the receiving room through paths other than the window. To further diminish effects due to flanking, the sound pressure levels provided by the horn were concentrated mostly around the window area (Fig. 5).

**Insertion loss measurements.** Insertion loss of the window is defined as the difference between the sound pressure level in the receiving room caused by noise source in the source room without and with the window installed. The sound pressure level in the receiving room was measured by a microphone in one of the corners of the room opposite from the window. Assuming hard-walled boundary conditions, all room modes will have their highest sound pressure amplitudes in the corners. The sound pressure level at the receiver microphone measured without the window installed includes the effects of acoustic mode shapes and absorption in the receiver room, the directivity of the noise source, and flanking through the particle board structure. When the window is installed, the sound pressure level at the receiver microphone includes all of these effects plus the effect of sound blocked by the window. Thus, the insertion loss is a measure of the sound transmitted through the window. To obtain a measure of the sound incident on the window, the sound pressure level was recorded at the location of the window without the window installed. The ratio of this "incident" sound pressure level and the insertion loss is an approximation of the ratio of incident and transmitted power, which is the definition of transmission loss. To verify the validity of this approach, a thin acrylic panel with a surface density of  $3.78 \text{ kg/m}^2$  was installed onto the support panel and separated along its edges by a thin layer of silicone rubber to simulate simply supported boundary conditions. Transmission loss obtained from the measured insertion loss and the "incident" sound pressure level of this panel is compared with calculated transmission loss for normal and field sound incidence. In the higher frequency region, where its behavior is governed by its surface mass  $m$ , this transmission

loss is represented by<sup>11</sup>

$$R \approx 10 \log[1 + (\omega m / 2\rho c)^2] \quad (2)$$

Above the 200 Hz one-third octave band, the measured transmission loss registers in between the calculated transmission loss for normal and field incidence of the incoming sound, as shown in Fig. 7. For values over 12 dB, the normal incidence mass law is 5 dB higher than the field incidence mass law. This shows that the transmission loss approximated by measured insertion loss and "incident" pressure is comparable with the theoretical transmission loss. Using this procedure, the transmission loss of the two window designs was determined and compared with their respective normal incident mass laws in Fig. 7. At the one-third octave band center frequencies of 200 and 500 Hz, the transmission loss is considerably lower than expected from mass law behavior. As discussed in the previous section, double/triple wall resonances degrade the transmission loss properties of the two windows at 196 and 516 Hz. Single-pane resonances occurring in the frequency range of interest do not strongly affect the transmission loss.

#### Intensity

**Test configuration.** For the intensity measurements, each of the windows was installed in a 1.22- × 1.52-m fuselage sidewall panel. A stiff mounting frame was designed and installed in the fuselage sidewall panel to accommodate each of the windows. The sidewall panel consists of a 0.114-cm-thick aluminum skin reinforced by four 15.2-cm-high frames with a spacing of 48.3 cm and eight 3.42-cm-high stringers with a spacing of 15.2 cm. These stiffeners divide the fuselage panel into 21 equal-area bays. The fuselage panel was tested with and without a trim treatment installed. The treatment consists of a 0.93-cm-thick viscoelastic layer attached to the skin and a 7.62-cm-thick layer of fiberglass supported by a trim panel, separated by an airgap of 6.65 cm (Fig. 8). The viscoelastic layer has a surface mass of 13.1 kg/m<sup>2</sup> and consists of a 0.29-cm-thick loaded urethane elastomer bonded to 0.64-cm-thick rubber. The trim panel is a combination of a 0.64-cm-thick Plexiglass panel adhered to a high strength-to-weight sandwich panel with laminated fiberglass facings and a core of blended plastic resins. In this configuration, the treatment directly behind the window has been removed and replaced by a transparent 0.25-cm-thick acrylic scratch shield attached to the trim panel leaving a spacing of 9.47 cm. The trim panel is decoupled from the window and sidewall to prevent structural flanking paths.

**Intensity measurements.** The intensity measurements were accomplished with a four-microphone probe to obtain the intensity vector in three-dimensional space. The 50-mm distance between the microphone centers was chosen to minimize errors caused by residual phase and cross-channel phase differences in the frequency range of interest. The probe and its orientation with respect to the panel are depicted in Fig. 9, where positive *x* axis is perpendicular to the back of the fuselage panel. The positive *y* axis is pointing up whereas *z* axis is in the horizontal direction, and both the *y* and *z* axes are parallel to the plane of the fuselage skin panel.

It can be shown that, for a separation distance  $\Delta r$  that is small compared with the wavelength, the intensity vector component in the direction *r* can be calculated from<sup>12</sup>

$$I_r = -(1/2\rho\Delta r) \overline{(p_A + p_B) \cdot (p_B - p_A)} dt \quad (3)$$

requiring sound pressure levels from two microphones. The quantity  $I_r$  is referenced to an intensity of 1 pW/m<sup>2</sup>. The measured intensity was corrected by a phase compensation function to adjust for the cross-channel phase difference between both channels of a microphone pair. Phase compensation functions between two channels having the same input signal were calculated from the imaginary and real parts of the

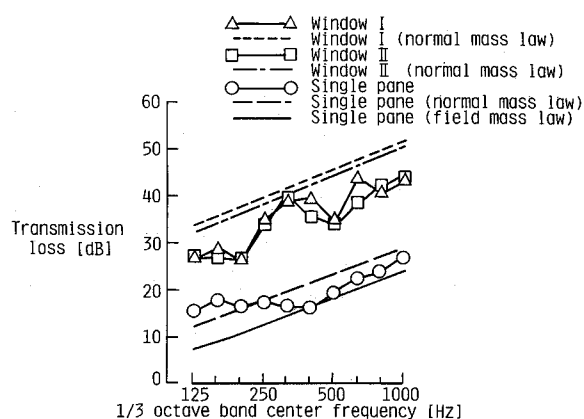


Fig. 7 Measured and predicted transmission loss for the two window designs and a single acrylic pane.

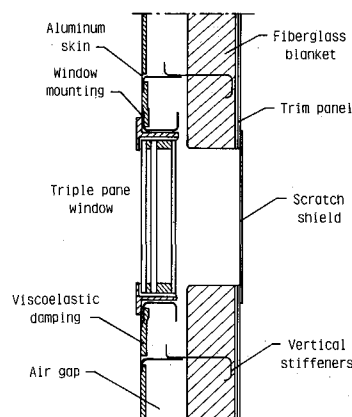


Fig. 8 Cross section of fuselage sidewall structure with the window and acoustic treatment installed.

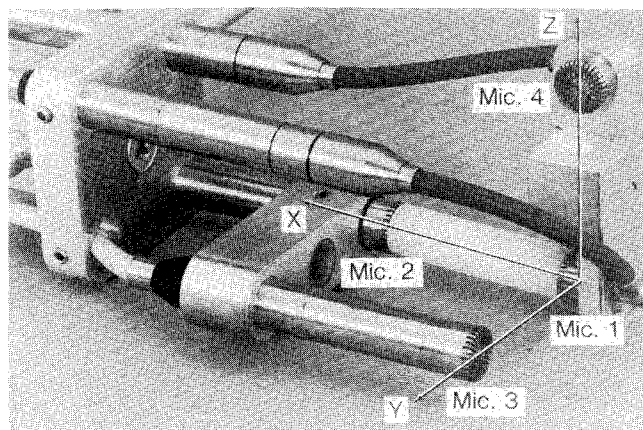


Fig. 9 Four-microphone intensity probe with related Cartesian coordinate system.

cross spectrum

$$\Delta\phi = \arctan(\text{Im } G_{AB} / \text{Re } G_{AB}) \quad (4)$$

To aid in data acquisition, data processing, and data management, a computer-aided test system was used. Intensity measurements were conducted on both sides of the fuselage panel at the center of each of the 21 bay areas. An additional four measurements were taken from inside the corners of the win-

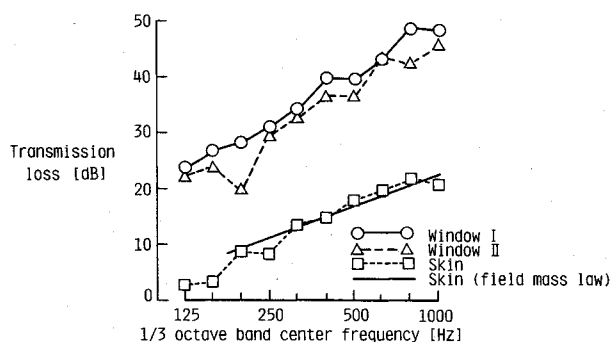


Fig. 10 Measured transmission loss for the fuselage skin and the two window designs using the three-dimensional intensity method.

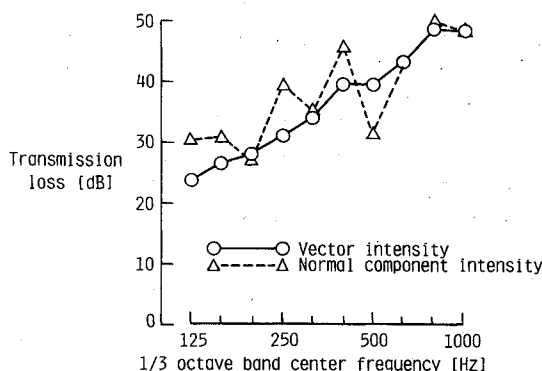


Fig. 11 Transmission loss of window I using three-dimensional vector intensity and normal component intensity methods.

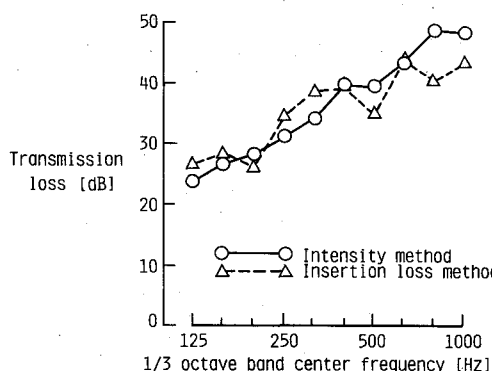


Fig. 12 Transmission loss of window I using the insertion loss and vector intensity methods.

down to provide more accuracy and detail in that area. On the source side of the fuselage, panel measurements were conducted 2.54 cm from the skin surface. At the receiving side, measurements were carried out in a plane 0.5 cm from the back side of the window for the case where no trim was installed and in a plane 0.5 cm from the transparent acrylic scratch panel for the case of the treated fuselage panel.

The normalized random error in the measurements was established by measuring the Reactivity Index, which is defined as the difference in intensity level  $L_I$  and sound pressure level  $L_P$ . It is related to the wave number  $k$ , the actual phase  $\phi$ , and the microphone spacing  $\Delta r$  by

$$L_K = L_I - L_P = -10 \log(k\Delta r/\phi) \quad (5)$$

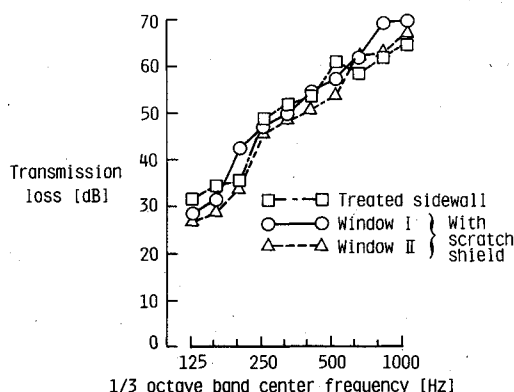


Fig. 13 Transmission loss (vector intensity method) of the treated sidewall and the window designs with a scratch shield installed.

The Reactivity Index was determined at the 25 measurement locations; results indicated that the normalized random error in each one-third octave band between 160 and 1000 Hz (68% confidence interval) was less than 1 dB for a phase mismatch of 0.3 deg and a 50-mm microphone spacing.<sup>13</sup>

The transmission loss of the bare fuselage skin panel obtained by the intensity vector method was compared with its field-incidence mass law transmission loss in Fig. 10. Except for the 125-, 160-, and 250-Hz one-third octave bands, good agreement was found in the frequency range of interest. The mass law transmission loss for normal sound incidence would have been up to 5 dB higher, which suggests that sound is incident on the fuselage panel at angles other than normal. Also shown in Fig. 10 is the experimental transmission loss for windows I and II using the intensity vector method. Preference was given to the three-dimensional intensity method rather than the normal component of the intensity because of the directionality of the source and the complexity of the window designs and the treated sidewall. In a thin homogeneous material, the impedance change does not substantially affect the directivity of the sound. The incident intensity vector and the transmitted intensity vector have the same direction, and their ratio is the same as the ratio of their normal components. For the triple-pane window installed in the fuselage panel, the angle of the transmitted vector is different because of various impedance changes through the triple-pane window and the treated sidewall. In addition, the measured transmitted sound is not originating only from one point on the structure, but rather from several different sources on the panel. The inclusion of more sources smoothes out the transmission loss curves. A comparison between the three-dimensional vector intensity and its normal component is shown in Fig. 11 for window I. The normal component intensity transmission loss is showing the effects of double/triple wall resonances in the 200- and 500-Hz one-third octave bands measuring only contributions perpendicular to the window. As other sources contribute (reflections off the inside of the window frame, etc.), the relative effect of window resonances is reduced for the three-dimensional intensity transmission loss.

Reasonable agreement is obtained (within 4 dB) for the frequency region of interest (125–630 Hz) when this vector intensity method is compared with the insertion loss method (Fig. 12). After installation of the trim and the trim scratch shield, the transmission loss of window designs I and II was measured using the intensity method. (Fig. 13). The higher transmission loss for these configurations is not only because of the additional scratch shield but also because of the absorption by the fiberglass in the cavity between the trim panel and the fuselage skin. At the blade passage frequency and two overtones, the transmission loss of windows I and II plus scratch shields is less than the average of the treated sidewall.

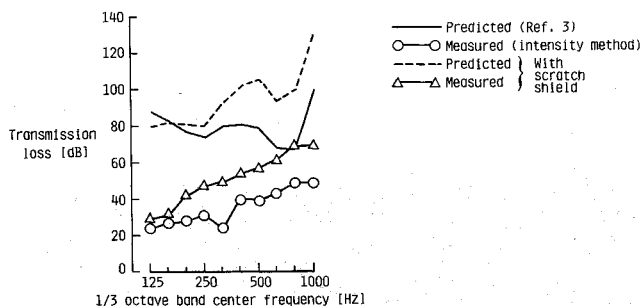


Fig. 14 Predicted<sup>3</sup> and measured transmission loss (vector intensity method) of window I with and without a scratch shield installed.

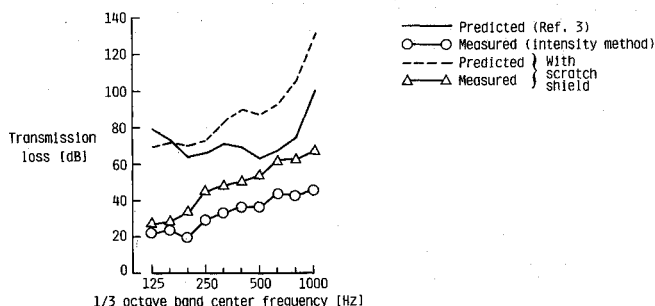


Fig. 15 Predicted<sup>3</sup> and measured transmission loss (vector intensity method) of window II with and without a scratch shield installed.

Finally, the measured transmission loss for windows I and II using the vector intensity method is compared with the predicted data from Ref. 3 in Figs. 14 and 15. At the blade passage frequency (164 Hz), measured data are about 50 dB lower than predicted. This disagreement may be attributed partially to differences in the assumptions made in the theoretical analysis and the laboratory conditions of the present study. In deriving the transmission loss at low frequencies, the theory assumes a specific acoustic impedance of the individual window panes that is proportional to their effective stiffness and inversely proportional to the frequency. Because the windows are designed to be installed in an aircraft fuselage sidewall, they will be dependent on the stiffness of that sidewall. This stiffness is limited and allows vibrations of the sidewall, reducing the effective stiffness of the windows assumed by the theory. The presence of lump mass resonances at 65 and 69 Hz, just below the frequency range of interest, allows for a rather rapid decrease in apparent transmission loss. Also, the theory assumes a plane wave incident on the window panes at a normal angle. This condition is not met in the current test setup although an attempt was made to approximate this condition by the use of a sound source horn close to the window pane surface. Angles of sound incidence different from normal degrade the transmission loss. A third explanation for the disagreement between theory and experiment is due to different calculated and measured window pane resonance frequencies. In this study, resonance frequencies were calculated using the actual dimensions of the window panes, which agreed with the measured resonance frequencies. In Ref. 3, the dimensions of the transparent pane area were chosen for calculation procedures, resulting in higher resonance frequencies for the window panes than measured (718 vs 558 Hz for the 0.94-cm-thick glass pane). This yields less transmission loss at frequencies below the fundamental resonance frequencies. For the combination of the window and the scratch shield, the predictions from Ref. 3 and the measured data from this study are in similar disagreement for analogous reasons.

## Conclusions

Experimental transmission loss was obtained for two window designs from Ref. 3 with and without a scratch shield using vector intensity and insertion loss techniques. The two experimental methods showed reasonable agreement. Both methods agreed closely with theoretical predictions for thin homogeneous panels that are believed to behave according to mass law in the frequency region of interest. It was shown that the combination of window plus the scratch shield provides less transmission loss than the average transmission loss of the treated fuselage sidewall panel at the blade passage frequency and the first two overtones. Double/triple wall resonances were shown to degrade the transmission loss characteristics of the two windows in the 200 and 500 Hz one-third octave bands. With the treatment and scratch shield installed, the degradation in transmission loss in these one-third octave bands was partially relieved. Experimentally obtained transmission loss of the two window designs disagreed considerably with the theoretical predictions in Ref. 3. Differences between actual measurements and assumptions in the theory were reason for part of this disagreement. Vibrating boundaries causing lump mass movement of the windows when installed in a fuselage sidewall diminishes the apparent stiffness of the panes. Assumptions of plane wave propagation and normal incidence could only be approximated in the current test setup. Individual panes responded in tests as if simply supported at the edges resulting in fundamental resonance frequencies that were lower than the resonances calculated in Ref. 3 where the edges of the transparent area were used. These differences degrade the transmission loss characteristics at frequencies below individual window pane resonances.

## Acknowledgments

This work was performed under NASA Contract NAS1-16978, Dr. C. A. Powell, technical monitor.

## References

- <sup>1</sup>Revell, J. D., Balena, F. J., and Koval, L. R., "Analytical Study of Interior Noise Control by Fuselage Design Techniques on High-Speed Propeller Driven Aircraft," NASA CR 159222, July 1978.
- <sup>2</sup>Prydz, R. A., Revell, J. D., Hayward, J. L., and Balena, F. J., "Evaluation of Advanced Fuselage Design Concepts for Interior Noise Control on High-Speed Propeller-Driven Aircraft," NASA CR 165960, Sept. 1982.
- <sup>3</sup>Prydz, R. A. and Balena, F. J., "Window Acoustic Study for Advanced Turboprop Aircraft," NASA CR 16441, Aug. 1984.
- <sup>4</sup>Grosveld, F., Navaneethan, R., and Roskam, J., "Noise Reduction Characteristics of General Aviation Type Dual Pane Windows," AIAA Paper 80-1874, Aug. 1980.
- <sup>5</sup>Vaicaitis, R., "Study of Noise Transmission Through Double Wall Aircraft Windows," NASA CR 172182, Oct. 1983.
- <sup>6</sup>Mixon, J. S., O'Neal, R. L., and Grosveld, F. W., "Investigation of Fuselage Acoustic Treatment for a Twin-Engine Turboprop Aircraft in Flight and Laboratory Tests," NASA TM 85722, Jan. 1984.
- <sup>7</sup>Grosveld, F. W., "Field-Incidence Noise Transmission Loss of General Aviation Aircraft Double-Wall Configurations," *Journal of Aircraft*, Vol. 22, Feb. 1985, pp. 117-123.
- <sup>8</sup>Leissa, A. W., "Vibration of Plates," NASA SP 160, 1969.
- <sup>9</sup>Cockburn, J. A. and Jolly, A. C., "Structural-Acoustic Response, Noise Transmission Losses and Interior Noise Levels of an Aircraft Fuselage Excited by Random Pressure Fields," Air Force Flight Dynamics Lab., TR-68-2, Wright-Patterson AFB, OH, Aug. 1968.
- <sup>10</sup>Grosveld, F. W., "Characteristics of the Transmission Loss Apparatus at NASA Langley Research Center," NASA CR 172153, May 1983.
- <sup>11</sup>Anonymous, "ASTM Standard Method for Laboratory Measurement of Airborne Sound Transmission Loss of Building Partitions," American Society for Testing Materials, Designation E90-81, *Annual Book of ASTM Standards*, Pt. 18, 1982.
- <sup>12</sup>Gade, S., "Sound Intensity (Part I. Theory)," *Technical Review*, Bruel & Kjaer Instruments, Denmark, No. 3, 1982.
- <sup>13</sup>Roland, J., "What Are the Limitations of Intensity Technique in a Semi-Diffuse Field," *Inter-Noise Proceedings*, 1982, pp. 715-718.